AMERICAN SOCIETY FOR MICROBIOLOGY | Molecular and Cellular Biology®

RESEARCH ARTICLE

DHX33 Interacts with AP-2β To Regulate *Bcl-2* Gene Expression and Promote Cancer Cell Survival

Jiuling Wang,[a,b] Weimin Feng,[a] Zhen Yuan,[b] Jason D. Weber,[c] Yandong Zhang[a]

[a]Department of Biology, Southern University of Science and Technology, Shenzhen, Guangdong, China
[b]SUSTech/UM Joint Ph.D. Program, Faculty of Health Sciences, University of Macau, Taipa, Macau, China
[c]ICCE Institute, Department of Medicine, Division of Molecular Oncology, Washington University School of Medicine, St. Louis, Missouri, USA

ABSTRACT The RNA helicase DHX33 has been found to be overexpressed in human cancers, where it promotes cancer development. Previous reports have shown that DHX33 deficiency caused cancer cell apoptosis, but the underlying mechanism remains unknown. In this study, we discovered that DHX33 regulates Bcl-2 family protein expression. In multiple human cancer cell lines, DHX33 was found to stimulate the transcription of *Bcl-2*. Mechanistically, we found that DHX33 interacts with the AP-2β transcription factor and acts as a coactivator to stimulate *Bcl-2* gene transcription. DHX33 deficiency abolished the loading of AP-2β onto the promoter of *Bcl-2* and thereby reduced the recruitment of active RNA polymerase II during transcription initiation. Acute knockdown of DHX33 in multiple human cancer cells caused decreased Bcl-2 protein level, which ultimately triggered mitochondrion-mediated cellular apoptosis. In addition, we found that normal human lung and mammary epithelial cells were less sensitive to acute DHX33 knockdown, implying that cancer cells are uniquely responsive to DHX33 reduction. These data support the notion that disruption of DHX33 function could be an important application for cancer therapy.

KEYWORDS apoptosis, BAD, *Bcl-2*, Bcl-2 family, DHX33, RNA helicase

The DEAD/DEAH box (DDX/DHX) helicases are involved in multiple aspects of RNA and DNA metabolism, including gene transcription, mRNA splicing/editing, ribosome RNA processing, mRNA export, RNA decay, mRNA translation and microRNA-induced gene silencing (1). They are characterized by their conserved structures that consist of two tandem domains (RecA1 and RecA2). Eight highly conserved helicase sequence motifs are arranged along two core domains that are critical for nucleic acid binding and ATP hydrolysis (2). After substrates bind to the helicase, the two core domains clench together, and the active ATPase sites are exposed for ATP hydrolysis, driving the remodeling of DNA/RNA-protein complexes (3). In addition to maintaining essential cellular processes, DDX/DHX proteins are known to be deregulated in human cancers (4). Accumulated evidence shows that cancer cells can employ numerous RNA helicases to promote cancer cell proliferation (5).

DHX33 is a member of the DEAH-box RNA helicase family proteins. We and others have previously identified DHX33 to be a critical player in cell proliferation and innate immunity (6–8). It was found to promote ribosome RNA synthesis (7), regulate protein translation (9), and associate with the promoters of genes involved in cell cycle regulation (10, 11). DHX33 promotes the recruitment of active RNA polymerase II on gene promoters to trigger cell cycle progression at all three checkpoints. DHX33 was additionally found to stimulate the transcription of MMP9, MMP14, and urokinase-type plasminogen activator (PLAU) to promote cancer cell migration (10). However, it

Citation Wang J, Feng W, Yuan Z, Weber JD, Zhang Y. 2019. DHX33 interacts with AP-2β to regulate *Bcl-2* gene expression and promote cancer cell survival. Mol Cell Biol 39:e00017-19. https://doi.org/10.1128/MCB.00017-19.

Address correspondence to Yandong Zhang, zhangyd@sustech.edu.cn.

Received 10 January 2019
Returned for modification 2 February 2019
Accepted 29 May 2019
Accepted manuscript posted online 10 June 2019
Published 12 August 2019

remains unclear whether DHX33 could serve as a coactivator or as a direct transcription factor to regulate gene expression.

Overexpression of DHX33 was found in several human cancers, such as lung, liver, lymphoma, and glioblastoma (10–13). Analysis of patients with non-small-cell lung cancer indicated that DHX33 is highly expressed in 30% (28/95) of cases (11). Elevated expression of DHX33 was also observed in 66.3% (345/520) of hepatocellular carcinoma patients, and low DHX33 expression correlated significantly with longer survival time (12). In human glioblastoma multiforme, DHX33 is highly expressed in 84% (80/95) of cases analyzed, while 39 cases of normal cerebral tissues were all negative for DHX33 expression (13). Several oncogenic signaling pathways have been found to regulate DHX33 expression. For instance, DHX33 is a downstream effector of oncogenic Ras^{V12} and is required for Ras^{V12}-induced cellular transformation (14). DHX33 expression is also regulated by c-Myc binding to the DHX33 promoter (10), further underscoring the integral relationship between DHX33 and known oncogenes.

Bcl-2 family proteins are important regulators of intrinsic apoptosis (15). Diverse intracellular stress signals act through Bcl-2 family proteins to induce activation of effector caspases. Bcl-2 family proteins can be divided into two categories, proapoptotic and antiapoptotic. Sensing intrinsic signals, Bax and Bak homo-oligomerize on the outer mitochondria membrane to trigger apoptosis through cytochrome *c* release (16). BH3-only proteins, such as BIM and PUMA, directly activate BAX, which can be reversibly inhibited by prosurvival proteins, such as Bcl-2, Bcl-xl, and Bcl-w (15, 16). The other BH3-only protein, BAD, indirectly activates BAK or BAX through competitively inhibiting Bcl-2 (17). In human cancers, Bcl-2 is frequently overexpressed (18). Although the relationship of Bcl-2 family members is well characterized, the upstream regulatory pathway driving the expression of Bcl-2 family proteins remains incompletely understood.

We and others have previously found that knockdown of DHX33 leads to apoptosis in human cancer cells (8, 11). However, the underlying mechanism of this process remains obscure. In this study, we reveal that DHX33 represses apoptosis through the direct upregulation of *Bcl-2* gene transcription. We identify that AP-2β is a binding partner for DHX33 and that DHX33 acts as a coactivator for AP-2β to promote the transcription of antiapoptotic *Bcl-2* gene. In addition, we found that normal human mammary and lung epithelial cells are less sensitive to DHX33 deficiency, indicating a unique and heightened sensitivity to DHX33 expression in cancer cells but not normal cells. Together, our data implicate the therapeutic potential of DHX33 in cancer treatment.

RESULTS

DHX33 supports breast cancer cell survival. We have previously observed that lung cancer cells rapidly undergo cell apoptosis after DHX33 knockdown. To investigate whether DHX33 promotes cell survival in other cancer cell types, we analyzed the effect of DHX33 knockdown in breast cancer cell lines. We applied several different shRNAs targeting DHX33 in BT549, HCC1806, and SKBR3 cells, respectively, with shScramble as a control. As shown in Fig. 1A and D, these shRNAs efficiently reduced DHX33 protein levels. DHX33 deficiency triggered cell death, as visualized by light microscopy of enhanced refractive cells (Fig. 1B and E). Through annexin V staining, we determined that these DHX33-deficient cells underwent apoptosis (Fig. 1C). To evaluate the effect of DHX33 knockdown in breast cancer cells *in vivo*, we injected SKBR3 cells that expressed significantly reduced levels of DHX33 into immunocompromised mice. As shown in Fig. 1F and G, we found that DHX33 knockdown decreased the tumorigenicity of SKBR3 cells *in vivo*. It is clear from these results that DHX33 expression is critical to support cell survival in breast cancer cells.

The requirement of DHX33 expression in breast cancer cell survival indicates that DHX33 might be somehow deregulated in breast cancers. To evaluate DHX33 expression levels in breast cancer cells, we first performed immunoblot analysis by employing a panel of breast cancer cell lines, with the noncancerous MCF10A cell line as a control.

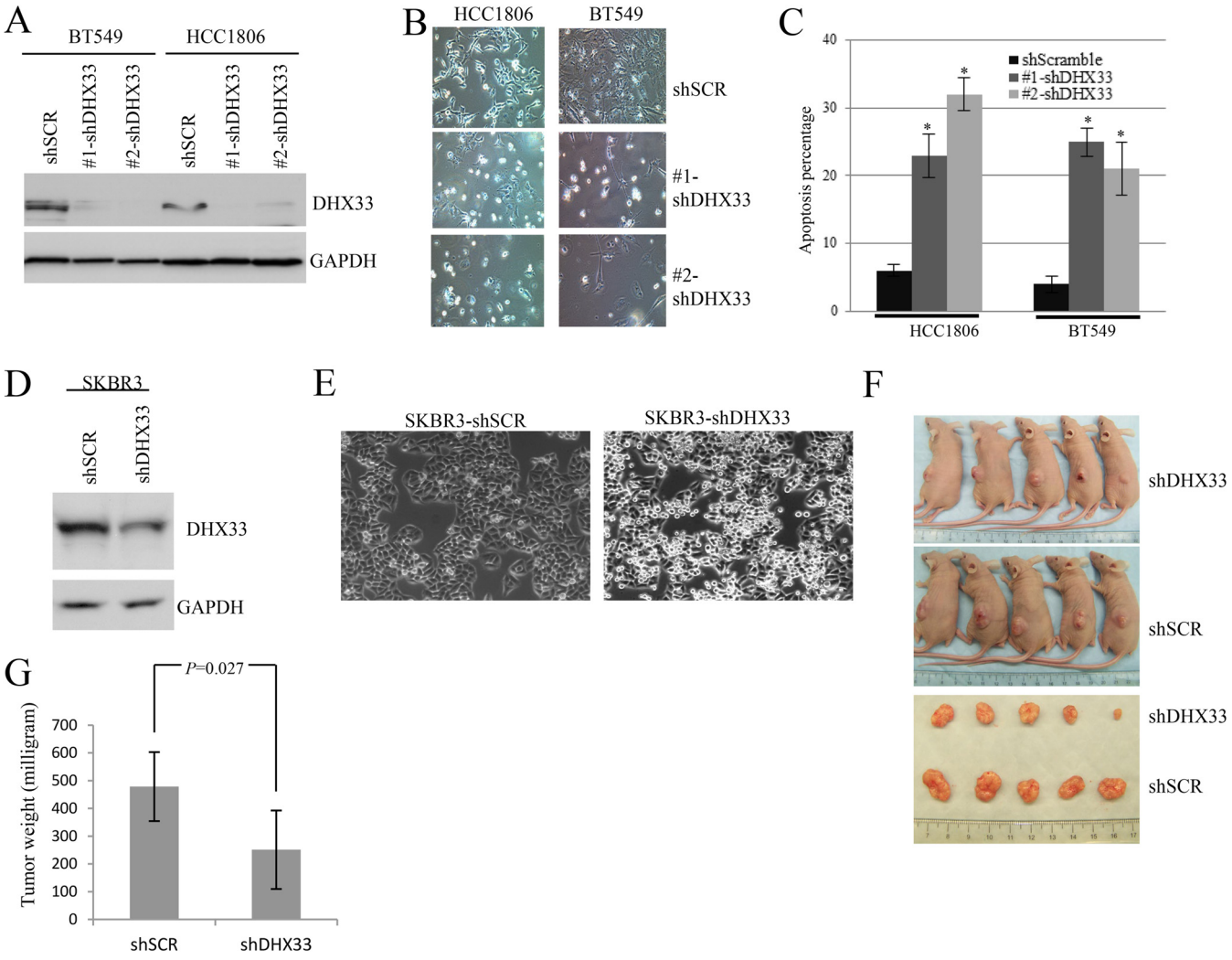

FIG 1 DHX33 supports breast cancer cell survival. (A and D) BT549 and HCC1806 (A) or SKBR3 (D) breast cancer cells were transduced with either shSCR or shRNA-DHX33 lentivirus. At 4 days postinfection, the cells were subjected to Western blot analysis with anti-DHX33 antibody; GAPDH served as an internal control. (B and E) At 5 days postinfection, images were taken using a phase-contrast microscope. After DHX33 knockdown, obvious cell death was observed. Typical images are shown at 10× magnification. (C) The cells described above were subjected to apoptosis analysis by flow cytometry using a Vybrant apoptosis kit after PI labeling of nuclei and FITC labeling of annexin V. Quantitation of apoptotic cells was calculated and graphed. Bars stand for the SD from three separate analyses. *, $P < 0.01$ ($n = 3$). (F) A group of five nude mice were injected in the flank on one side with SKBR3 cells transduced with either shSCR or with shDHX33 (10^6 cells per injection). Tumors were dissected after 3 weeks, and images were obtained before and after tumor removal. (G) Tumors were weighed; the values in each group were calculated as averages and SD. There is a statistical difference between these two groups.

As shown in Fig. 2A, we found DHX33 is highly expressed in many breast cancer cell lines compared to lower expression in MCF10A cells. We further investigated the expression of DHX33 in breast cancer tissues. As shown in Fig. 2B, the tissue microarray contains 40 cases of human ductal invasive breast cancer tissues with tumor adjacent normal tissues for control. The immunohistochemistry scores for cancer tissues are listed in Table 1. We found that 10 of 40 breast cancer tissues demonstrated highly positive staining for DHX33, while most tumor adjacent normal tissues displayed negative DHX33 staining.

DHX33 transcriptionally regulates *Bcl-2* family gene expression. To investigate the underlying mechanism for apoptosis induced by DHX33 reduction, we first analyzed the changes in total gene expression after DHX33 knockdown. As shown by RNA sequencing (RNA-seq) results in H1299 lung cancer cells (Fig. 3A), we found that genes involved in the mitochondrial pathway of apoptosis were highly deregulated. The mRNA levels of several Bcl-2 family members demonstrated altered expression after DHX33 knockdown. The *Bcl-2* gene itself was significantly downregulated whereas BAD,

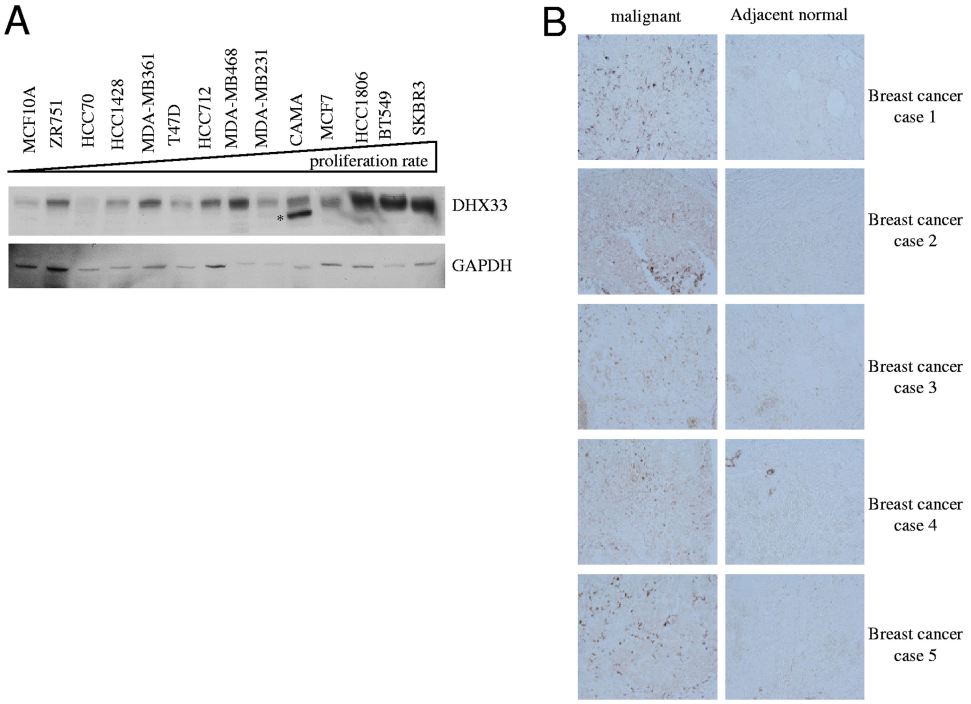

FIG 2 Deregulation of DHX33 protein in breast cancer cell lines and tumor tissues. (A) A panel of breast cancer cell lines was evaluated for the expression of DHX33 protein. These cancer cell lines were ordered in the proliferation rate, with MCF10A as a control. GAPDH was used as an internal control in Western blot analysis. *, short variant of DHX33 with a molecular mass of 54 kDa. (B) Immunohistochemistry was performed on a human tissue array, including 40 cases of invasive ductal carcinoma tissue specimens, with their adjacent normal specimens as controls. Five representative images of adjacent normal and malignant cancer tissues are shown. All images were obtained at a 10× magnification.

BIM, BMF, and PUMA genes were upregulated in H1299 cells after DHX33 knockdown. To check whether these results also occurred in other cell types, we further performed reverse transcription-PCR (RT-PCR) analysis for MDA-MB231 cells, BT549 cells, and MCF10A cells. As shown in Fig. 3B to D, after DHX33 knockdown, Bcl-2 was downregulated, BAD and BIM were upregulated in all three cell lines, whereas BMF, BAK, BOK, and BAX were upregulated in a cell-type-dependent manner. Interestingly, we observed that Bcl-xl, Bcl-w, and MCL1 were upregulated in different cell lines after DHX33 knockdown, implicating a possible feedback regulatory mechanism. To confirm the results from RNA-seq, we further performed immunoblot analysis for both lung cancer and breast cancer cells (Fig. 4A and B). Depending on the different cell lines, DHX33 knockdown dramatically altered the expression of at least one or multiple Bcl-2 family members, particularly *Bcl-2* gene expression. The altered expression of Bcl-2 family members caused pre-caspase 7 to be cleaved into caspase 7 (Fig. 4A and B) and PARP was also cleaved after DHX33 knockdown (Fig. 4A and B). To confirm the expression changes of Bcl-2 family members at the transcriptional level, RT-PCR analysis was further performed after DHX33 knockdown. As shown in Fig. 4C, we found that after DHX33 knockdown, *Bcl-2* gene transcription was downregulated in multiple human cancer cell lines, while the transcript levels of BAD, BIM, and BMF were elevated only in certain cell types, such as H1299 cells, but not in MDA-MB-231 cells. Deregulation of these important genes should cause oligomerization of BAX/BAK protein on the outer membranes of mitochondria, which in turn leads to mitochondrion-mediated apoptosis. We therefore analyzed the membrane potential of mitochondria after DHX33 knockdown in cancer cells with JC-1 staining. Under normal conditions, JC-1 will polymerize in the mitochondria, emitting red fluorescence. However, in apoptotic cells, due to mitochondrial collapse, JC-1 will stay in the cytosol as monomers to emit green fluorescence. As shown in Fig. 4D and E, we found that DHX33 knockdown in cancer

TABLE 1 Clinical data of breast cancer cases and the immunohistochemistry staining results

Case	Staining strength	% positive cells	Score	Pathology diagnosis
1	1	1	2	Invasive lobular carcinoma
2	1	2	3	Invasive lobular carcinoma
3	1	3	4	Medullary carcinoma
4	1	2	3	Invasive ductal carcinoma
5	1	1	2	Invasive ductal carcinoma
6	1	1	2	Invasive ductal carcinoma
7	1	3	4	Invasive ductal carcinoma
8	1	2	3	Invasive ductal carcinoma
9	2	2	4	Invasive ductal carcinoma
10	3	3	6	Invasive ductal carcinoma
11	2	3	5	Invasive ductal carcinoma
12	1	1	2	Invasive ductal carcinoma
13	1	1	2	Invasive ductal carcinoma
14	2	2	4	Invasive ductal carcinoma
15	1	2	3	Invasive ductal carcinoma
16	1	2	3	Invasive ductal carcinoma
17	1	1	2	Invasive ductal carcinoma
18	0	0	0	Invasive ductal carcinoma
19	1	1	2	Invasive ductal carcinoma
20	1	2	3	Invasive ductal carcinoma
21	1	2	3	Invasive ductal carcinoma
22	1	1	2	Invasive ductal carcinoma
23	0	0	0	Invasive ductal carcinoma
24	1	2	3	Invasive ductal carcinoma
25	0	0	0	Invasive ductal carcinoma
26	1	3	4	Invasive ductal carcinoma
27	1	2	3	Invasive ductal carcinoma
28	1	1	2	Invasive ductal carcinoma
29	2	1	3	Invasive ductal carcinoma
30	2	1	3	Invasive ductal carcinoma
31	2	1	3	Invasive ductal carcinoma
32	1	3	4	Invasive ductal carcinoma
33	1	2	3	Invasive ductal carcinoma
34	1	3	4	Invasive ductal carcinoma
35	0	0	0	Invasive ductal carcinoma
36	1	2	3	Invasive ductal carcinoma
37	2	1	3	Invasive ductal carcinoma
38	1	3	4	Invasive ductal carcinoma
39	0	0	0	Invasive ductal carcinoma
40	0	0	0	Invasive ductal carcinoma

cells caused an increase in JC-1 monomers, indicating depolarization of the mitochondrial membrane to favor apoptosis.

AP-2β is a binding partner for DHX33 that associates with the promoter of the *Bcl-2* gene. To investigate the underlying molecular mechanism for how DHX33 might alter *Bcl-2* gene transcription, we performed mass spectrometry to identify potential binding partners for DHX33. We immunoprecipitated DHX33 in two different systems: one was to immunoprecipitate endogenous DHX33 by anti-DHX33 antibody, and the other was to immunoprecipitate exogenous FLAG-tagged DHX33 by anti-FLAG antibody (both systems used IgG as immunoprecipitation controls). As shown in Table 2, we found several transcription factors as binding partners for DHX33 from these two different immunoprecipitation complexes but not in the control IgG samples. Among these transcription factors, activator protein 2 (AP-2) appeared to be a promising binding partner for DHX33. We therefore obtained antibodies for AP-2α and AP-2β, as well as for the transcription factors Pur-α and Pur-β, for further analysis. We initially used anti-FLAG antibody to immunoprecipitate DHX33 from cell lysates in H1299 and Calu-1 cells and then performed immunoblot analysis for the identified transcription factors. As shown in Fig. 5A and B, we found that only AP-2β was confirmed to be a binding partner for DHX33, while AP-2α, Pur-α, and Pur-β had no interaction with DHX33 in these cancer cells. The interaction between AP-2β and DHX33 was also

A

	Gene name	sh-Scrambled	#2-shDHX33
BH3-only proteins	BIM(BCL2L11)	833.425	1736.55
	PUMA(BBC3)	275.993	472.987
	BAD	503.868	1710.33
	BIK	252.388	290.396
	HRK	51.7486	79.6404
	BMF	1649.6	2206.62
	BID	1897.45	1415.07
Pro-survival proteins	BCL-2(BCL2)	123.47	42.7339
	BCL-XL(BCL2L1)	4930.64	4179.18
	BCL-W(BCL2L2)	1562.65	1871.75
	MCL1	23052.6	14833.5
	A1(BCL2A1)	0.90787	4.85612
	BCL-B(BCL2L10)	0	0
Pro-apoptotic proteins	BAX	1033.16	719.678
	BAK(BAK1)	2071.76	2375.62
	BOK	1894.72	1437.41

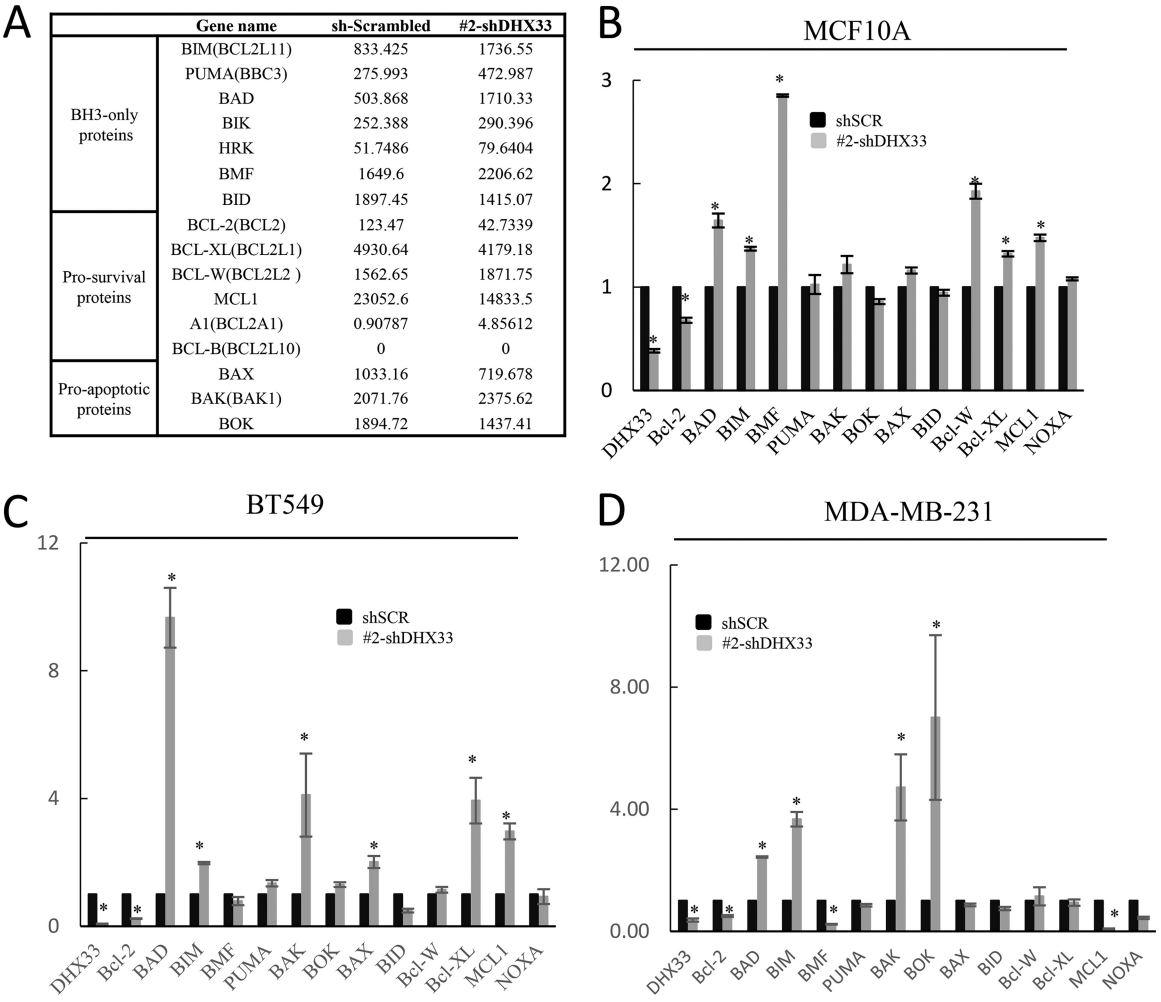

FIG 3 Bcl-2 family genes were deregulated in DHX33-deficient cells. (A) RNA-seq result from H1299 cells that were transduced with shRNA or shDHX33 lentivirus. A group of genes were selected for mRNA level comparison; these genes were grouped based on their functions in the intrinsic apoptosis pathway. (B) MCF10A cells were transduced with either shSCR or shRNA-DHX33 lentiviruses. At 4 days postinfection, total RNA was extracted and subjected to RT-PCR analysis for Bcl-2 family genes. *, $P < 0.05$ ($n = 3$). (C and D) Breast cancer cell lines, BT-549 (C) and MDA-MB-231 (D), were transduced with either shSCR or shRNA-DHX33 lentiviruses. At 4 days postinfection, total RNA was extracted and subjected to RT-PCR analysis for Bcl-2 family genes. *, $P < 0.05$ ($n = 3$).

detected in the breast cancer cell line MDA-MB231 and noncancerous MCF10A cells (Fig. 5C and D). Next, we further performed immunoprecipitation for endogenous DHX33 in cancer cells with anti-DHX33 antibody. As shown in Fig. 5E, endogenous DHX33 was found to associate with AP-2β. A previous report demonstrated that AP-2α was able to directly repress *Bcl-2* gene expression (19). We hypothesized that DHX33 and AP-2β may form a complex that binds to the gene regulatory region of *Bcl-2*. We therefore performed chromatin immunoprecipitation (ChIP). As shown in Fig. 5F and G, we found that the DHX33 protein associated with the promoters of Bcl-2 family members, including Bcl-2, BAD, BIM, and BMF. Through ChIP analysis, we further discovered that AP-2β also associated with the promoter of the *Bcl-2* gene (Fig. 5H). To investigate whether DHX33 and AP-2β simultaneously bind to the same Bcl-2 promoter, we further performed (re-chromatin immunoprecipitation (reChIP) analysis, as shown in Fig. 5I, and we found that DHX33/AP-2β complex can bind to the same Bcl-2 promoter region. These data are consistent with the notion that AP-2β and DHX33 bind to each other to form a transcriptional regulatory complex for the *Bcl-2* gene.

AP-2β and DHX33 cooperate in the regulation of the *Bcl-2* gene. To further understand this AP-2β-DHX33 complex, we knocked down AP-2β in lung cancer cells

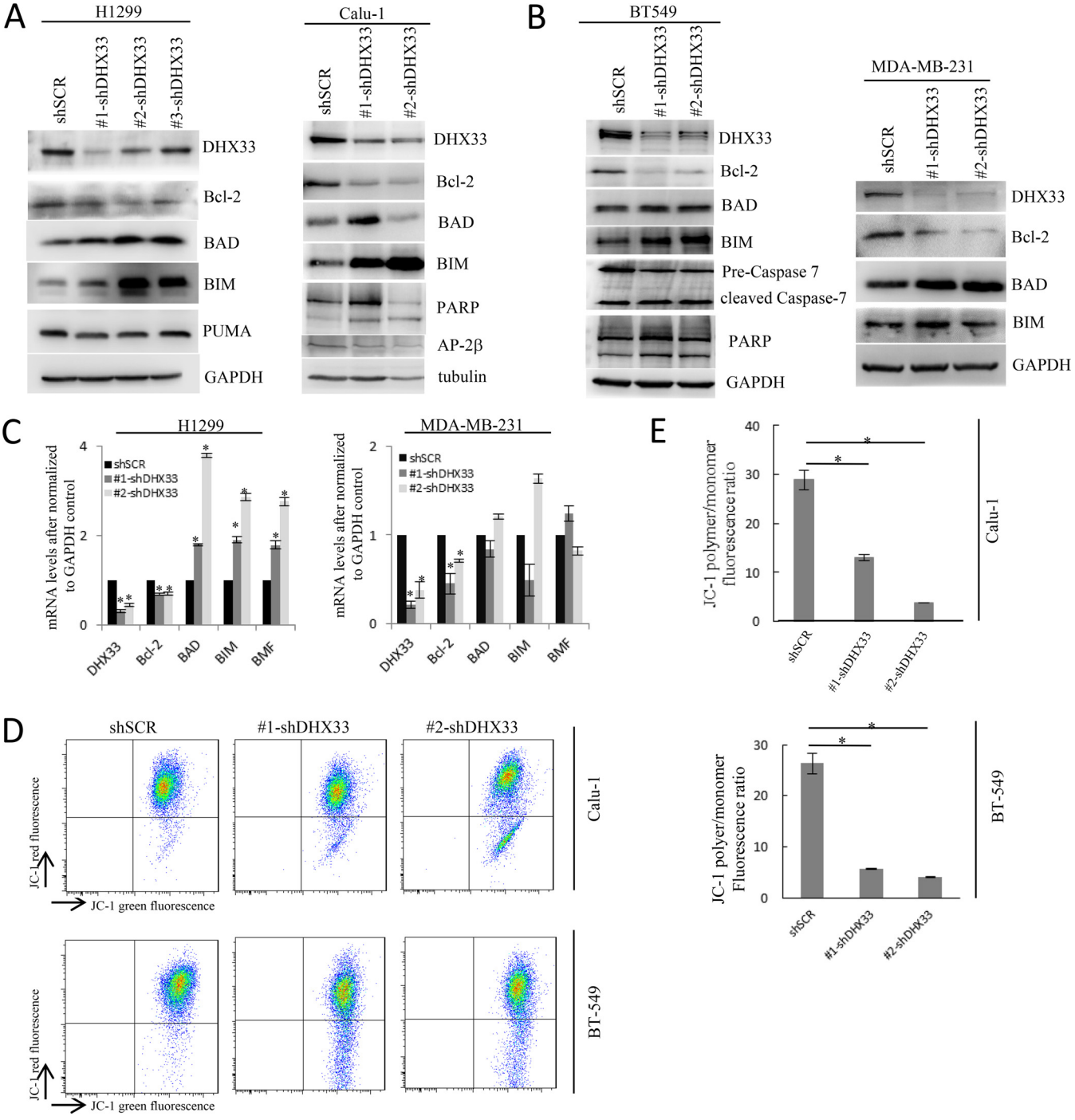

FIG 4 DHX33 transcriptionally regulates Bcl-2 family genes. (A and B) The lung cancer cell lines H1299 and Calu-1 or the breast cancer cell lines BT-549 and MDA-MB-231 were transduced with either shSCR or shRNA-DHX33 lentiviruses. At 4 days postinfection, the cells were subjected to Western blot analysis with the indicated antibodies for Bcl-2 family members. GAPDH or tubulin was used as an internal control. (C) H1299 lung cancer cells or MDA-MB-231 breast cancer cells were infected with two different shRNAs targeting DHX33, with shSCR as a control. At 4 days after lentiviral infection, the cells were harvested. Total RNA was extracted and reverse transcribed into cDNA, and qPCR was performed on these cells with the indicated primers. Bars represent the SD from three independent analyses. All show statistically significant changes compared to the scramble control. *, $P < 0.05$ ($n = 3$). (D) Calu-1 and BT549 cells were transduced by lentivirus encoding either shSCR or shDHX33. At 4 days postinfection, the cells were subjected to JC-1 mitochondrial membrane potential analysis. After JC-1 staining, the cells were analyzed by using a flow cytometer with an excitation wavelength of 488 nm and emission wavelengths of 529 and 590 nm, respectively. Red fluorescence signals represent polymers of JC-1 in mitochondria, while green fluorescence signals represent JC-1 monomers in the cytosol. (E) Quantitation of the JC-1 polymer/monomer fluorescence ratio after DHX33 knockdown in Calu-1 and BT-549 cells. An increase in JC-1 monomer indicates mitochondrial depolarization. *, $P < 0.01$ ($n = 3$).

TABLE 2 Protein-binding partners of DHX33 identified by mass spectrometry[a]

Analysis and accession no.	Description	Score	Coverage	No. of:					Size (kDa)	Calculated pI
				Proteins	Unique peptides	Peptides	PSMs	AAs		
Immunoprecipitation with anti-FLAG antibody										
Q9H6R0	Putative ATP-dependent RNA helicase DHX33 OS=*Homo sapiens* GN=DHX33 PE=1 SV=2 - (DHX33_HUMAN)	28.55	15.70	3	13	13	15	707	78.8	8.91
O95782	AP-2 complex subunit alpha-1 OS=*Homo sapiens* GN=AP2A1 PE=1 SV=3 - (AP2A1_HUMAN)	4.67	4.40	2	3	4	4	977	107.5	7.03
E9PR62	AP-2 complex subunit alpha-2 OS=*Homo sapiens* GN=AP2A2 PE=1 SV=1 - (E9PR62_HUMAN)	2.75	5.56	7	1	2	2	378	41.9	8.98
A0A087X253	AP-2 complex subunit beta OS=*Homo sapiens* GN=AP2B1 PE=1 SV=1 - (A0A087X253_HUMAN)	4.58	3.29	12	3	3	3	913	101.3	5.29
A0A087WY71	AP-2 complex subunit mu OS=*Homo sapiens* GN=AP2M1 PE=1 SV=1 - (A0A087WY71_HUMAN)	2.56	11.52	4	3	3	3	434	49.5	9.54
Immunoprecipitation with anti-DHX33 antibody										
A0A0D9SFB3	ATP-dependent RNA helicase DDX3X OS=*Homo sapiens* GN=DDX3X PE=1 SV=1 - (A0A0D9SFB3_HUMAN)	11.59	57.02	7	5	5	6	114	12.6	9.55
O95782	AP-2 complex subunit alpha-1 OS=*Homo sapiens* GN=AP2A1 PE=1 SV=3 - (AP2A1_HUMAN)	13.11	29.27	2	4	4	5	123	14.5	11.05
A0A087WYD1	AP-2 complex subunit beta (Fragment) OS=*Homo sapiens* GN=AP2B1 PE=1 SV=1 - (A0A087WYD1_HUMAN)	13.05	22.57	5	11	11	12	669	69.4	9.67
A0A087WY71	AP-2 complex subunit mu OS=*Homo sapiens* GN=AP2M1 PE=1 SV=1 - (A0A087WY71_HUMAN)	12.83	7.92	2	7	7	7	947	107.1	8.79
P53680	AP-2 complex subunit sigma OS=*Homo sapiens* GN=AP2S1 PE=1 SV=2 - (AP2S1_HUMAN)	12.71	26.57	16	10	10	10	493	54.9	9.67

[a]PSMs, posttranslational modifications; AAs, amino acids.

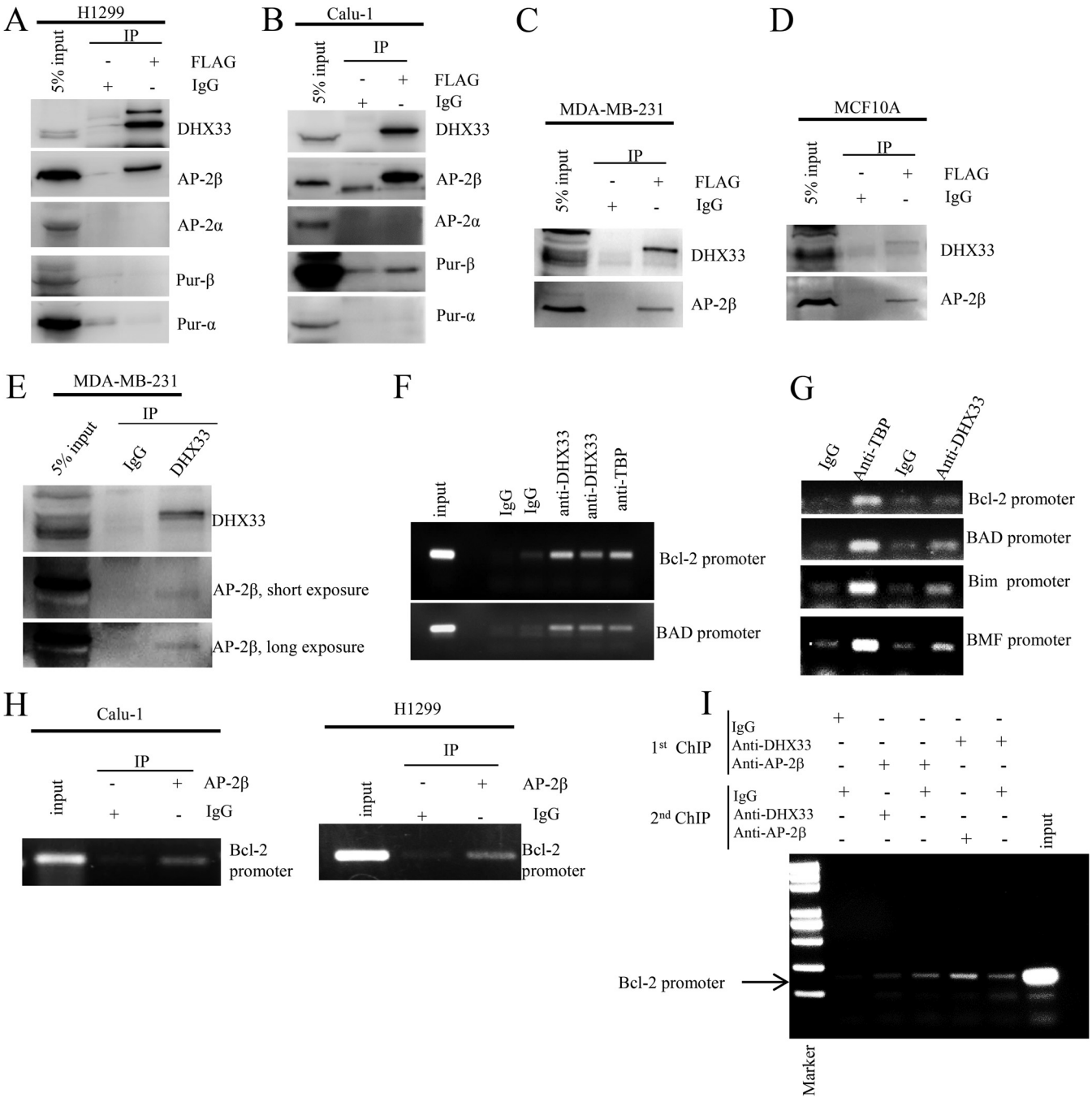

FIG 5 AP-2β is a binding partner for DHX33 that associates with the promoter of the *Bcl-2* gene. (A and B) H1299 (A) or Calu-1 (B) cells were transduced with lentivirus encoding either empty vector or wild-type FLAG-tagged DHX33. At 4 days postinfection, the cells were subjected to IP analysis with anti-FLAG antibody; IgG was used as a control. Western blot analysis was performed to analyze each of the indicated proteins. (C and D) MDA-MB231 (C) or MCF10A (D) cells were transduced with lentivirus encoding either empty vector or wild-type FLAG-tagged DHX33. At 4 days postinfection, the cells were subjected to IP analysis with anti-FLAG antibody; IgG was used as a control. Western blot analysis was performed to analyze each of the indicated proteins. (E) MDA-MB231 cells were immunoprecipitated with anti-DHX33 antibody (A-3, Santa Cruz Biotech). Immunoprecipitated complexes for endogenous DHX33 were then detected by Western blot analysis with anti-AP-2β antibody. (F and G) Calu-1 (F) or H1299 (G) cells were subjected to ChIP analysis. Anti-DHX33 antibody was used, with anti-TATA-binding protein (TBP) as a positive control and IgG as a negative control. Chromatin fragments after IP were then PCR amplified with the designated primers from BAD and Bcl-2 gene promoters. (H) Calu-1 and H1299 cells were subjected to ChIP analysis. Anti-AP-2β antibody was used, with IgG as a negative control. Chromatin fragments were then analyzed by PCR with Bcl-2 promoter primers. (I) MDA-MB231 cells were transduced with lentivirus encoding wild-type DHX33-FLAG. Cells were then subjected to reChIP analysis. The first IP experiment was performed with anti-DHX33 antibody or anti-AP-2β antibody, while the second IP was performed with the other antibody. It is easy to detect reChIp signal with anti-DHX33 since the first ChIP antibody is followed by anti-AP-2β as the second antibody.

and then analyzed cell apoptosis. As shown in Fig. 6A, we designed several shRNAs to knock down endogenous AP-2β expression. After successfully reducing AP-2β expression with two different shRNAs, we observed a significant increase in lung cancer cell apoptosis (Fig. 6B and C). To analyze whether the induction of cell apoptosis could be through a mitochondrial pathway, we further analyzed the protein levels of Bcl-2 family genes, including Bcl-2, BAD, and BIM, as shown in Fig. 6A. We found that only Bcl-2 was significantly downregulated, whereas BAD and BIM had no significant changes at the protein level. We further found that Bcl-2 transcription was diminished as shown by the RT-PCR result in Fig. 6D. We did not observe a consistent change of mRNA levels for BAD and BMF. The mRNA level of BIM had a moderate decrease in AP-2β knockdown cells. Induction of apoptosis after AP-2β knockdown was observed not only in lung cancer cells but also in breast cancer cell lines (Fig. 6E and F). However, noncancerous MCF10A cells appeared to tolerate AP-2β deficiency. We found that AP-2β knockdown caused the Bcl-2 protein to be downregulated in cancer cell lines, whereas the levels of BAD and BIM were not influenced. Interestingly, we found that AP-2β knockdown caused DHX33 protein levels to be markedly increased compared to the control (Fig. 6A and F). To determine whether there was a reciprocal regulation between AP-2β and DHX33, we further analyzed AP-2β protein levels in DHX33 knockdown cells. As shown in Fig. 6G, AP-2β level did not undergo marked change after DHX33 knockdown in H1299 cells, SK-LU1 cells, and Calu-1 cells (Fig. 4A, right panel).

It is likely that DHX33 is required for AP-2β to stimulate *Bcl-2* gene transcription. We therefore performed ChIP in cancer cells after DHX33 knockdown to analyze the recruitment of AP-2β onto the *Bcl-2* gene promoter. As shown in Fig. 6H, we found that DHX33 deficiency significantly reduced the loading of AP-2β onto the promoter of the *Bcl-2* gene. DHX33 deficiency further reduced the loading of phosphorylated RNA polymerase II onto the *Bcl-2* promoter (Fig. 6I). Moreover, AP-2β knockdown in cancer cells dramatically reduced the recruitment of activated RNA polymerase II on the Bcl-2 promoter (Fig. 6J), while the loading of DHX33 onto Bcl-2 promoter was enhanced, possibly due to an increase in the absolute amount of DHX33 protein levels (Fig. 6J).

Expression of DHX33 protects cells from drug-induced apoptosis. In drug-induced cell apoptosis, proapoptotic proteins, such as PUMA and p53, are significantly upregulated. During severe DNA damage in cells, we found that DHX33 protein levels were downregulated, as shown in Fig. 7A. To analyze the effect of wild-type DHX33 in drug-induced apoptosis, we first expressed DHX33 protein, as shown in Fig. 7B. Overexpression of DHX33 protein indeed promoted cell survival, as shown in Fig. 7C and D. We further performed protein expression analysis for cells that were treated with these drugs after wild-type DHX33 was overexpressed. For comparison, we used the K94R helicase-defective DHX33 mutant. As shown in Fig. 7E, we found that wild-type DHX33 lowered the expression of proapoptotic genes, such as BAD and BIM, while the DHX33 K94R mutant failed to do so. Wild-type DHX33 reduced cancer cell apoptosis compared to K94R mutant DHX33 (Fig. 7F and G). To check whether DHX33 regulation of Bcl-2 is dependent on its helicase activity, we analyzed the mRNA levels of Bcl-2 in H1299 cells. For both vehicle and etoposide treatment samples, we found Bcl-2 upregulation was observed in wild-type DHX33 samples comparing to the helicase-defective mutant samples (Fig. 7H). This indicates that the helicase activity of DHX33 is required for gene regulation of Bcl-2.

Normal epithelial cells demonstrate less apoptosis after DHX33 knockdown. To study the effect of DHX33 deficiency on normal epithelial cells, we first chose MCF10A cell line for analysis. After infecting MCF10A cells with shRNA lentiviruses targeting DHX33, MCF10A cells were incubated in fresh medium in the presence of puromycin to select for the infection-positive cells. Two days after selection, the remaining cells with puromycin resistance were harvested. Immunoblotting was performed to analyze protein expression, as shown in Fig. 8A. DHX33 protein levels were decreased with simultaneous downregulation of Bcl-2. Cyclin B2 served as a control since it has been shown to be positively regulated by DHX33. To examine the effect of DHX33 depletion

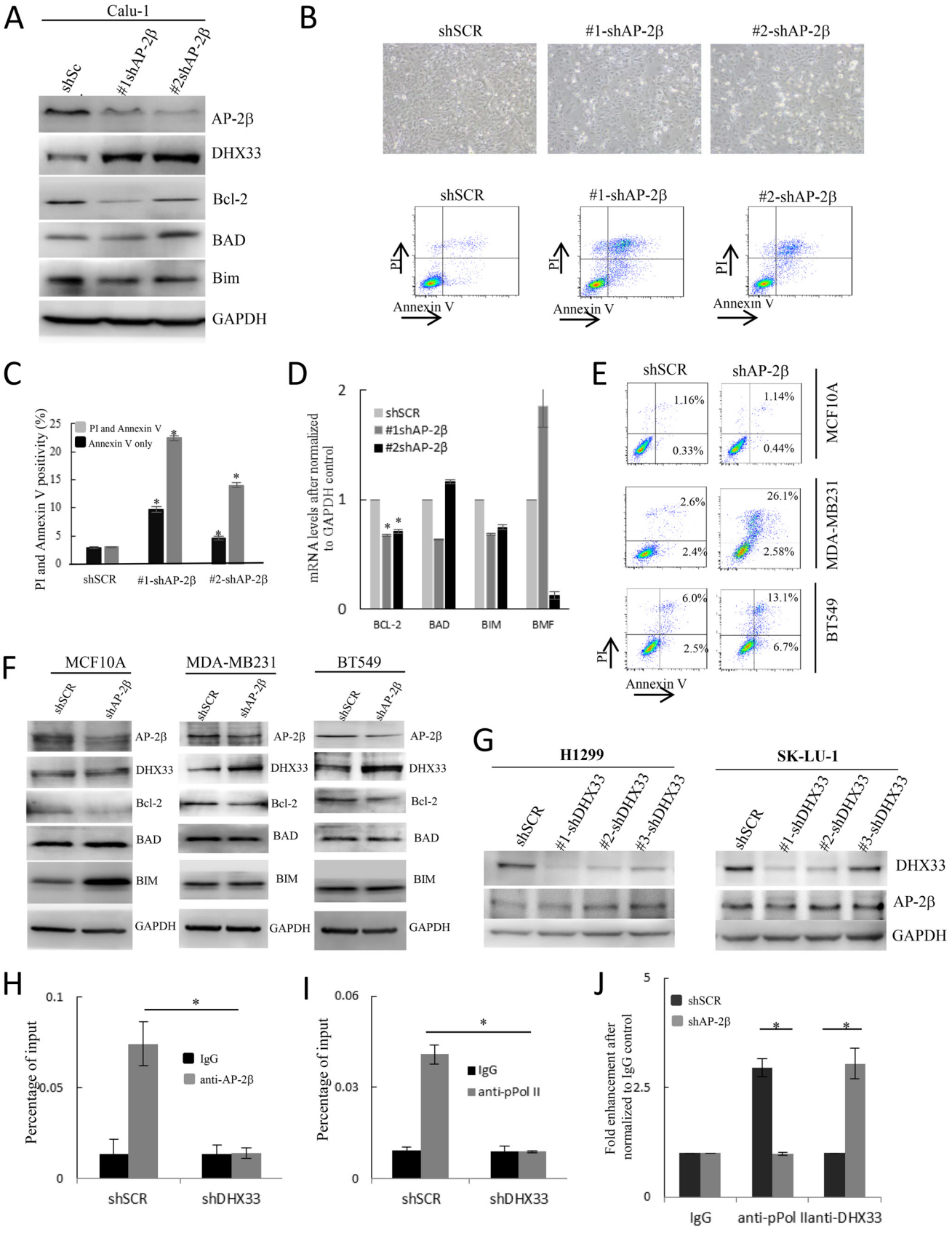

FIG 6 AP-2β and DHX33 cooperate in regulation of the *Bcl-2* gene. (A) Calu-1 cells were infected by lentivirus encoding either scramble shRNA or shAP-2β. At 4 days postinfection, cell lysates were analyzed by Western blotting with anti-AP-2β, anti-DHX33, anti-Bcl-2, anti-BAD, and anti-BIM antibodies. GAPDH

(Continued on next page)

on cell proliferation and apoptosis of MCF10A cells, DHX33-depleted cells were subjected to fluorescence-activated cell sorting (FACS) analysis for cell cycle distribution and annexin V-propidium iodide (PI) analysis. Profiles of DHX33-depleted MCF10A cells are shown in Fig. 8B. We observed cell cycle arrest in these cells after DHX33 knockdown. However, only a mild increase from 1 to 3% of apoptosis was observed in DHX33-depleted MCF10A cells compared to the control (Fig. 8B to D). We further performed a similar analysis using BeaS2B, an immortalized human lung epithelial cell line. As shown in Fig. 8E, DHX33 was successfully knocked down using shRNA lentiviruses. In this cell line, no apparent changes in BAD and Bcl-2 were observed. Similar to MCF10A cells, DHX33 knockdown caused BeaS2B cell cycle arrest at the G_1/S transition (Fig. 8F), but with no significant observable cell death (Fig. 8F to H), again underscoring the dramatically different responses between cancerous and normal cells to DHX33 reduction.

DISCUSSION

In this study, we identified a novel functional complex between AP-2β and DHX33 in *Bcl-2* gene regulation and found that DHX33 is a coactivator of AP-2β to stimulate *Bcl-2* gene transcription. Transcription factor AP-2 has been found to play important roles in embryonic development, cell differentiation, and cell survival (20). The AP-2 protein family includes three different members: AP-2α, AP-2β, and AP-2γ (21–24). All three AP-2 members share a highly conserved helix-span-helix motif in the C terminus that is responsible for protein dimerization and DNA binding (25). The sequence of their DNA-binding domain is unique and does not resemble those from other transcription factors (26). A palindromic region which is GC-rich has been found to be a preferential site for AP-2 protein dimer (25). AP-2 DNA transactivation domain contains a proline-rich region in the amino terminus and an adjacent acidic region. Mechanistically, these two domains have distinct activity to recruit RNA polymerase II in order to regulate gene expression (25). The three AP-2 isoforms have different DNA transactivation sequences and thus different functions in regulating cellular activities (20). This is supported by the different phenotypes observed in AP-2α and AP-2β gene knockout mice even though the embryonic expression patterns of AP-2α and AP-2β overlap significantly (27). Mice deficient for AP-2α develop cranioabdominoschisis and defects in multiple tissues/organs, while none of this is observed in AP-2β-null mice (28, 29). AP-2β knockout leads to autosomal-recessive polycystic kidney disease due to aberrant apoptosis after Myc induction (30).

At the level of primary amino acid sequence, AP-2β and AP-2α have 72% sequence identity and 82% positivity. Their DNA binding domains are exactly the same as shown in Fig. 9 (31). The core domain of AP-2, which is involved in DNA binding, was found to be a region spanning amino acid residues 252 to 260. This sequence is identical between AP-2α and AP-2β. They primarily differ by the DNA transactivation domains, especially in the acidic region. Previous studies have shown that overexpression of AP-2α caused cell apoptosis through binding to the *Bcl-2* promoter to repress its transcription (19). In the present study, however, we found that AP-2β functions quite differently in cancer cells. AP-2β promotes the transcription of the *Bcl-2* gene through

FIG 6 Legend (Continued)
served as an internal control. (B) The cells mentioned above were further subjected to FACS analysis after PI-annexin V staining. The percentage of cells in each quadrant is shown. Typical pictures of cell morphology were obtained. (C) Quantitation of apoptotic cells. The percentages of early apoptosis and late apoptosis were calculated. *, $P < 0.01$ ($n = 3$). (D) For the cells described above, total RNAs were extracted and subjected to quantitative RT-PCR analysis for expression changes of Bcl-2 family genes. *, $P < 0.01$ ($n = 3$). (E) MCF10A, MDA-MB231, and BT549 cells were separately infected by lentivirus encoding either scramble shRNA or shAP-2β. At 4 days postinfection, the cells were subjected to FACS analysis after PI-annexin V staining. The percentage of the cells in each quadrant is shown. (F) The cells were subjected to Western blot analysis with the indicated antibodies. GAPDH served as an internal control. (G) H1299 and SK-LU-1 cells were infected by lentivirus encoding either scramble shRNA or three different shRNAs targeting human DHX33. At 4 days postinfection, cell lysates were collected and subjected to Western blotting with anti-AP-2β and anti-DHX33 antibodies; GAPDH was used as an internal control. (H) Calu-1 cells were infected by lentivirus encoding either shSCR or shRNA targeting DHX33. At 4 days postinfection, the cells were subjected to ChIP analysis with anti-AP-2β antibody, using IgG as a control. Data were plotted against the percentage of input. *, $P < 0.01$ ($n = 3$). (I) For these cells, a similar ChIP was performed with anti-pPol II antibody, with IgG as a control. Data were plotted against the percentage of input. *, $P < 0.01$ ($n = 3$). (J) Calu-1 cells were infected by lentivirus encoding either shSCR or shRNA targeting AP-2β. At 4 days postinfection, the cells were subjected to ChIP analysis with anti-pPol II and anti-DHX33 antibodies, with IgG as a control. Data were plotted against percentage of input. *, $P < 0.01$ ($n = 3$).

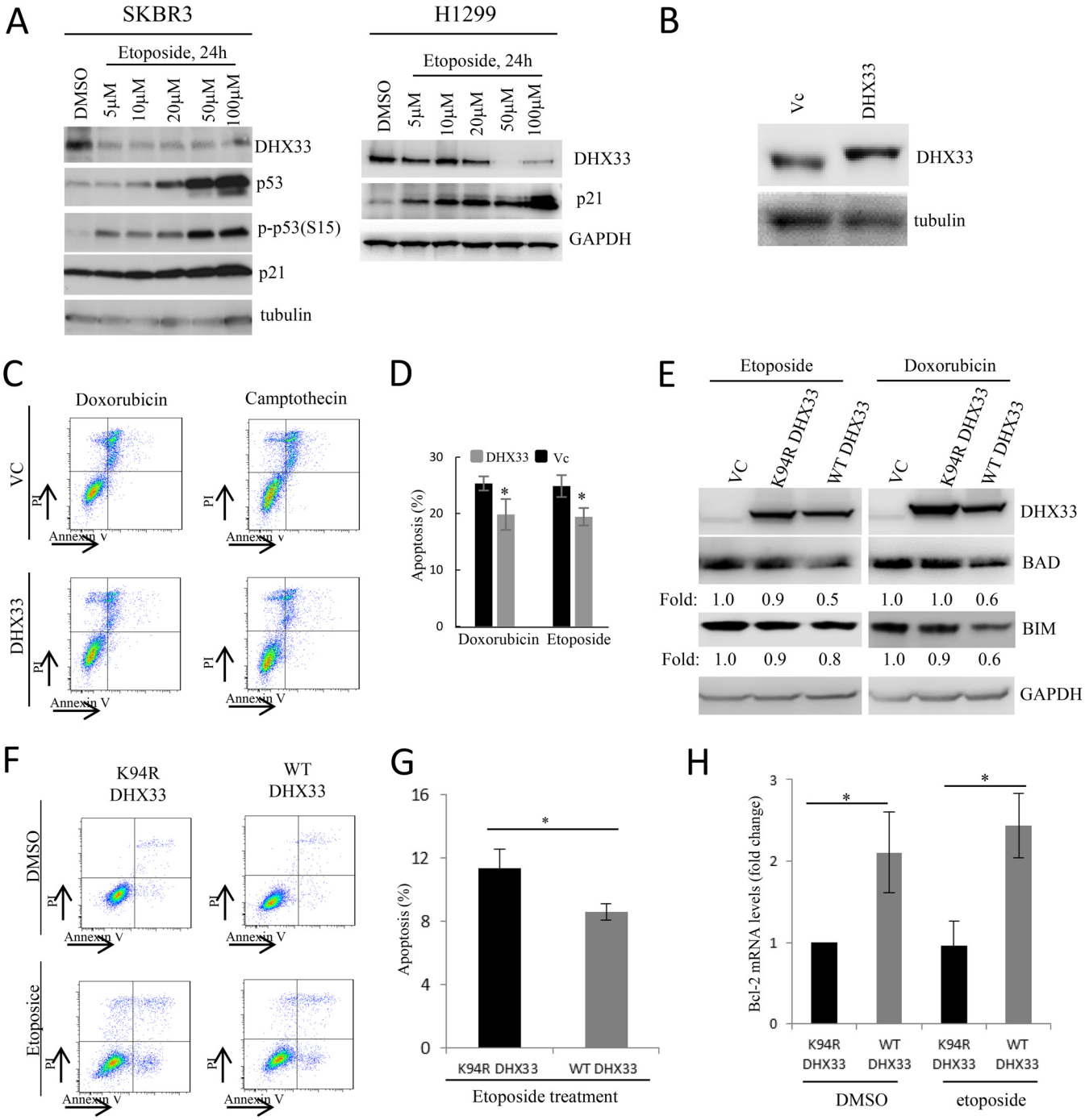

FIG 7 Expression of DHX33 protects cells from drug-induced apoptosis. (A) SKBR3 cells (left) and H1299 cells (right) were treated with etoposide at different concentrations for 24 h. Cell lysates were then subjected to Western blotting with the indicated antibodies. (B) H1299 lung cancer cells were infected with lentivirus encoding either wild-type FLAG-tagged DHX33 or empty vector. At 4 days after lentivirus infection, the cells were analyzed by Western blotting for the DHX33 protein expression. Tubulin was used as a control. (C) The cells described above were treated with drugs (0.1 μM doxorubicin or 10 nM camptothecin) for 72 h. The supernatant and the adherent cells were collected and stained with FITC-PI. Stained cells were analyzed by flow cytometry. The percentage of cells is shown in each quadrant. (D) An apoptosis index is displayed in a bar chart. *, $P < 0.05$ ($n = 3$). (E) H1299 cells were further transduced by lentivirus encoding either empty vector, wild-type DHX33, or a helicase dead mutant DHX33 (K94R). After 72 h, the cells were treated with etoposide (50 μM) or doxorubicin (5 μM) for 24 h. Drug-treated cells were further subjected to Western blotting with the indicated antibodies. (F) H1299 cells were transduced by lentivirus encoding either wild-type DHX33 or helicase dead mutant DHX33 (K94R). After 72 h, the cells were treated with etoposide (50 μM) for 24 h; dimethyl sulfoxide served as a control. The cells were collected and stained with FITC-PI. Stained cells were analyzed by flow cytometry. The percentage of cells is shown in each quadrant. (G) An apoptosis index is displayed in a bar chart. *, $P < 0.05$ ($n = 3$). (H) Total RNA was extracted from the above-mentioned cells. The mRNA levels of Bcl-2 were detected by RT-PCR analysis after normalization to a GAPDH control. *, $P < 0.05$ ($n = 3$).

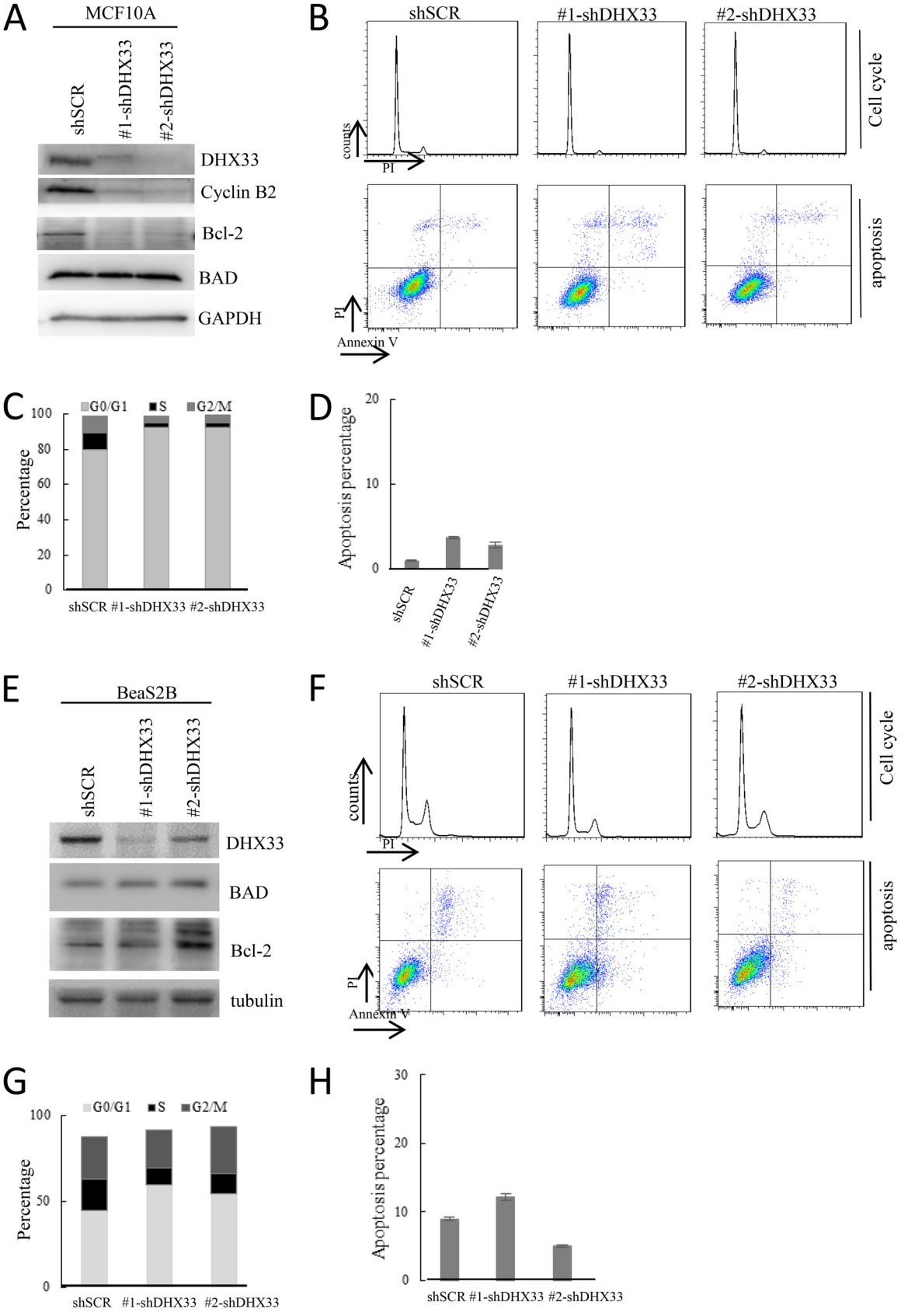

FIG 8 Normal human epithelia demonstrate less apoptosis after DHX33 knockdown. (A and E) Normal cell lines MCF10A (A) and BEAS-2B (E) were infected with lentivirus encoding either shSCR or shDHX33. At 4 days postinfection by lentivirus, the protein levels of DHX33,

(Continued on next page)

FIG 9 Sequence alignment between AP-2α and AP-2β and comparison for their structural domains. (A) Structural domains in AP-2α and AP-2β proteins. The AP-2 transactivation domain is located in the N terminus, specifically including a proline-rich domain and an acidic domain. The C terminus includes a highly conserved DNA-binding domain and an AP-2 dimerization domain. (B) Sequence alignment between AP-2α and AP-2β protein sequences. The blue box denotes the DNA-binding region; within this region, a red box denotes the critical amino acid sequence of AP-2 involved in DNA binding. A green box denotes the AP dimerization domain.

direct binding to *Bcl-2* gene promoter, thereby recruiting activated RNA polymerase II to initiate *Bcl-2* transcription; this unique AP-2β activity is highly dependent on its association with DHX33. DHX33 deficiency leads to a reduced loading of AP-2β onto the promoter of Bcl-2 and therefore reduces the recruitment of RNA polymerase II. Our results suggest that DHX33 acts as a coactivator of AP-2β in regulating gene expression. Given that the DNA binding domain is highly conserved between AP-2β and AP-2α, it is possible that these two proteins competitively inhibit each other to regulate *Bcl-2* gene transcription, resulting in either cell survival or apoptosis.

AP-2β has been found to be abnormally expressed in multiple human cancers (32, 33). Evidence shows that AP-2β upregulates multiple genes such as MMP-2, MMP-9, c-Jun, p-ERK, and STAT3 to promote cancer proliferation, migration, and survival (34). Despite these efforts, AP-2β remains a poorly defined transcription factor. Our study provides a novel molecular mechanism for the function of AP-2β in cell survival. The

FIG 8 Legend (Continued)
Bcl-2, BAD, and cyclin B2 were analyzed by Western blotting with the indicated antibodies. GAPDH or tubulin was used a control. (B and F, top rows) For the above-mentioned cells, at 4 days postinfection, the cells were collected and fixed by 75% ethanol. The cells were then treated with PI. Stained cells were analyzed by flow cytometry for the cell cycle spectrum. (B and F, bottom rows) At 5 days after infection, the cells were all collected and then stained with FITC-PI. Stained cells were subjected to flow cytometry. The percentage of cells is shown in each quadrant. (C and G) Quantitation of percentages for G_1, S, and G_2 phases. (D and H) Quantitation for the apoptosis index.

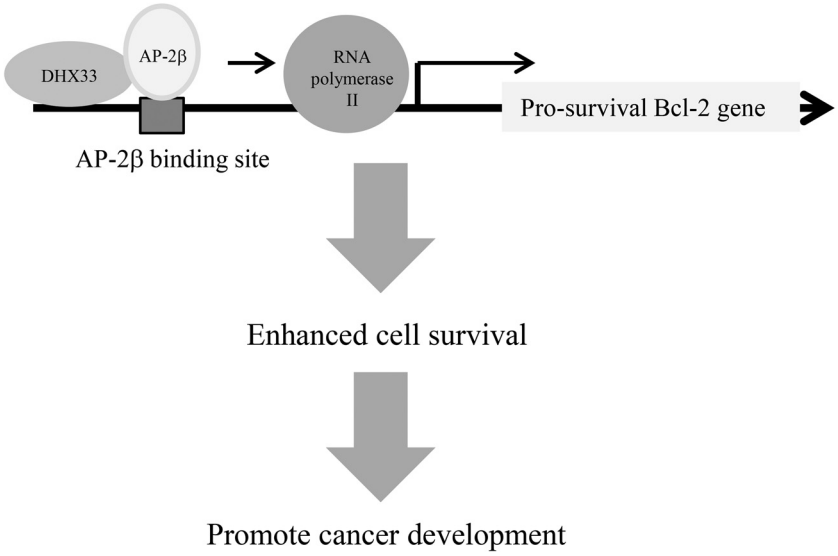

FIG 10 Graphic summary. A diagram shows how DHX33 works together with AP-2β to regulate *Bcl-2* gene transcription. This causes cancer cell survival, which contributes to tumorigenesis.

function of AP-2β may not be limited to promoting cancer cell survival since DHX33 has also been shown to be involved in other cellular activities. Therefore, it should be worthwhile to study whether this novel DHX33-AP-2β functional complex regulates the expression of other genes. A genomewide analysis should provide more clues regarding the importance of this complex in controlling targeted gene expression.

In this study, we also found that DHX33 protein binds to other gene promoters, such as BAD, BIM, and BMF genes, even though this appears to occur in a cell-type-dependent manner. The mechanism for how DHX33 might regulate these genes remains to be elucidated. It is possible that DHX33 acts as a coactivator or corepressor through its association with other transcription factors to modulate the expression of a variety of genes. Regardless, any regulation is likely to require the enzymatic activity of DHX33, given our findings that a helicase-defective mutant of DHX33 failed to influence *Bad* and *Bim* gene expression. It is interesting that DHX33 was found to bind to GC-rich regions in both RNA-seq and ChIP-seq analyses (data not shown). It may be worthwhile to further investigate how the helicase activity of DHX33 is involved in gene regulation. Genomewide ChIP, coupled with transcriptome analysis, should provide better clues.

Overall, our study for the first time delineates the novel role of DHX33 in regulating cancer cell apoptosis. We demonstrated that DHX33 binds to and cooperates with the AP-2β transcription factor to promote the expression of the prosurvival *Bcl-2* gene, leading to cancer cell survival (Fig. 10). Our data also show that in normal lung and mammary epithelial cells, DHX33 loss did not cause marked cell death, which contrasts with the higher sensitivity of cancer cells to DHX33 deficiency. The differential sensitivity to DHX33 loss between normal and cancer cells might be explored as a novel treatment for human cancers. Since reactivation of apoptosis is a basic principle in anticancer therapy, it is worthwhile to further explore the effect of DHX33 inhibition in cancer cells for potential cancer treatment.

MATERIALS AND METHODS

Lentivirus production. To produce lentivirus, pLKO.1-shRNA and virus packaging plasmid pCMV-VSV-G and pCMVΔR8.2 were transfected into HEK293T cells by Lipofectamine 2000 reagent (Life Technologies). The shRNA sequences targeting human DHX33 were used previously (9). The shRNA sequences targeting human AP-2β were (from 5′ to 3′) #1-shAP2β (CGGTTCTTTCGAGTTTAGTAA) and #2-shAP2β (GCGTACAACGGAGCAACAATA). To produce lentivirus overexpressing DHX33, pLVX-FLAG-tagged wild-type DHX33 or K94R mutant DHX33 and packaging plasmids pCMV-VSV-G with pCMVΔR8.2

were cotransfected into HEK293T cells. After 48 h, the culture supernatant was collected and centrifuged at 2,000 rpm for 2 min. Virus was then aliquoted and frozen at −80°C.

Western blotting and immunoprecipitation. For Western blot analysis, cells were lysed by radioimmunoprecipitation assay (RIPA) buffer supplemented with protease and phosphatase inhibitors (Thermo Fisher). After incubation for 10 min on ice, cell lysates were further disrupted by sonication. Whole-cell extract was then subjected to SDS-PAGE, with a loading amount of 50 μg of protein per sample. Proteins were then transferred onto a polyvinylidene difluoride membrane. Membranes were blocked in 5% nonfat milk, which was diluted in 1× Tris-buffered saline–Tween (TBST) buffer for 1 h at room temperature. Primary antibodies diluted in 5% fetal bovine serum (FBS; diluted in 1× TBST) were incubated with the membrane at 4°C overnight. Membranes were then rinsed with 1× TBST buffer for multiple times and incubated with horseradish peroxidase-labeled secondary antibodies in 5% FBS (diluted in 1× TBST) at room temperature for 2 h. Blots were visualized with an ECL kit (Thermo Fisher).

For immunoprecipitation, cells were lysed using EBC cell lysis buffer supplemented with protease and phosphatase inhibitors (Thermo Fisher). After incubation for 10 min on ice, cell lysates were further disrupted by sonication. Whole-cell lysates were centrifuged at 13,000 rpm for 10 min at 4°C. Supernatants were adjusted to a concentration of approximately 1 mg/ml and incubated with 2 μg of indicated antibody overnight at 4°C; normal IgG was used as a control. The next day, protein A/G-conjugated beads were added, and cell lysates were further incubated for 1 to 2 h at 4°C. Beads were then washed with EBC buffer three times before analysis.

The following antibodies were used: anti-DHX33 (A-3 for immunoprecipitation [IP] analysis) and anti-DHX33 (B-4 for immunohistochemistry and Western blot analysis), Santa Cruz Biotechnology (sc-390574 and sc-390573); anti-DHX33 for Western blot analysis, Bethyl [A300-800A] and anti-AP-2β (for Western blot analysis), Cell Signaling Technology (2509S); anti-AP-2β (for IP analysis), ABclonal (A7935); anti-AP-2α, Abcam (ab108311); anti-Pur-α, Bethyl (A303-543A-T); anti-Pur-β, Bethyl (A303-650A-T); anti-pPOL II (phosphorylation on S2 for ChIP analysis), Abcam (ab-5095); anti-TBP (for ChIP analysis), Santa Cruz Biotechnology (sc-204); anti-Bcl-2, Cell Signaling Technology (4223S); anti-BAD, Santa Cruz Biotechnology (sc-8044); anti-BIM, Cell Signaling Technology (2933S); anti-PUMA, Abcam (ab33906); anti-GAPDH, Absin (abs830030); and anti-FLAG (M2) antibody, Sigma (F1840).

Quantitative real-time PCR. The primers were all designed by using the Integrated DNA Technologies (IDT, Inc., Coralville, IA) online real-time PCR tool and purchased from BGI (Shenzhen). Total RNA was extracted by using a HighPure RNA isolation kit (Roche) and then transcribed into cDNA by using a PrimeScript mix kit (TaKaRa). Real-time PCR is performed with an ABI One-Step plus cycler that is managed with the corresponding software. To analyze mRNA levels, SYBR green Supermix (Bio-Rad) was used, and transcript quantification was calculated by using the $\Delta\Delta C_T$ value after normalization to the GAPDH (glyceraldehyde-3-phosphate dehydrogenase) values. A melting curve was used to confirm the amplification of a single product. The primer sequences used for quantitative real-time PCR analyses are presented in Table 3.

MitoProbe JC-1 assay. Calu-1 cells were infected with lentivirus encoding either scramble shRNA or shDHX33. At 4 days postinfection, 10^6 cells were resuspended in 1 ml of warm complete medium and transferred into 12-well plates. JC-1 was added to a final concentration of 2 μM, and cells were incubated at 37°C with 5% CO_2 for 30 min. The cells were then rinsed once with phosphate-buffered saline (PBS) and resuspended with 500 μl of PBS. Finally, cells were analyzed by a flow cytometer with a 488-nm excitation wavelength and 529-nm/590-nm emission wavelengths. The MitoProbe JC-1 assay kit was obtained from Thermo Fisher (catalog no. M34152).

Mass spectrometry. Calu-1 cells with or without 3×FLAG-tagged DHX33-1 expression were lysed in EBC buffer (50 mM Tris-HCl, 120 mM NaCl, 1 mM EDTA) containing 1% NP-40, protease-phosphatase inhibitor cocktail, and 100 U/ml RNase inhibitor). The cells were then incubated on ice for 25 min. Insoluble material was removed by centrifugation. Equal amounts of lysates were incubated with 4 μg of anti-FLAG antibody (Sigma, F1840) or anti-DHX33 antibody (Bethyl, A300-799A), with IgG as a control. Magnetic beads were added into a lysate-antibody mixture, followed by incubation for 2 h at 4°C with rotation. Immunoprecipitates were then washed six times with EBC buffer. Beads were further washed three times with 50 mM NH_4HCO_3 before suspension in 50 μl of 50 mM NH_4HCO_3 containing 8 M urea. Dithiothreitol (DTT) was added to the beads at a final concentration of 10 mM. Samples were incubated at 30°C for 60 min before the addition of 2 μl of 0.5 M iodacetamide at room temperature for 30 min in the darkness. Then, 350 μl of 50 mM NH_4HCO_3 and 5 μl of trypsin/LysC (20:1) were added to the samples for digestion at 30°C overnight. Formic acid (8 μl) was added to the reaction mixture in a new tube, and the samples were allowed to evaporate for 6 to 8 h. Peptides were desalted by using a ZipTip C_{18} column and dried with a SpeedVac. The samples were then submitted for analysis with using liquid chromatography coupled mass spectrometry (Orbitrap Fusion) at the Southern University of Science and Technology.

Immunohistochemistry. Human breast cancer tissue microarrays were purchased from US Biomax. This tissue microarray contains 40 cases of lung cancer cases. Tissues were deparaffinized in xylene and rehydrated in a series of alcohol solution with decreasing concentrations. The antigen was retrieved in Tris buffer (pH 9.0) in a steamer. Tissues were then incubated in 1% H_2O_2 in methanol to extinguish endogenous peroxidase. After being blocked with 10% FBS for 1 h at room temperature, the tissues were incubated with primary antibody at 4°C overnight. Standard protocol was then followed using a Dako kit according to the manufacturer's recommendations. The staining intensity was then scored as follows based on criteria described previously (35): 0, no staining; 1, weak; 2, moderate; and 3, strong. The percentages of positively stained cells were rated 1, 2, or 3 if the values were $<$25%, 25 to 50%, or $>$50%, respectively. If the cumulative score was $\geq$4, the case was defined as a positive case.

TABLE 3 Primers used for quantitative real-time PCR

Primer	Sequence (5′–3′)
BIM-FP	TGGAGACGAGTTTAACGCTTAC
BIM-RP	CCGCAAAGAACCTGTCAATG
BMF-FP	ACCCCAGCGACTCTTTTATG
BMF-RP	TTTCGGGCAATCTGTACCTC
Bcl2-FP	ACTGGAGAGTGCTGAAGATTG
Bcl2-RP	AGTCTACTTCCTCTGTGATGTTG
BAD-FP	GACCTTCGCTCCACATCC
BAD-RP	AGTACTTCCGCCCATATTCAAG
GAPDH-FP	TGACAACGAATTTGGCTACA
GAPDH-RP	GTGGTCCAGGGGTCTTACTC
DHX33-FP	CGTCCTCCACAACCCTCCTT
DHX33-RP	AAAATTCTCTTTGCACCAATCCTT
NOXA-FP	GGAGATGCCTGGGAAGAAG
NOXA-RP	TGCCGGAAGTTCAGTTTGTC
PUMA-FP	CGACCTCAACGCACAGTAC
PUMA-RP	CCTAATTGGGCTCCATCTCG
BAX-FP	GACATGTTTTCTGACGGCAAC
BAX-RP	AAGTCCAATGTCCAGCCC
MCL1-FP	CCAAGGACACAAAGCCAATG
MCL1-RP	TGATGTCCAGTTTCCGAAGC
Bcl-w-FP	AACAAGGAGATGGAACCACTG
Bcl-w-RP	TCCCCGTATAGAGCTGTGAA
Bcl-xl-FP	GTGGAAAGCGTAGACAAGGAG
Bcl-xl-RP	CTGCATTGTTCCCATAGAGTTC
BID-FP	ATTAACCAGAACCTACGCACC
BID-RP	TGACCACATCGAGCTTTAGC
BAK-FP	AGAGTTCCAGACCATGTTGC
BAK-RP	GTAGCCGAAGCCCAGAAG
BOK-FP	GGCGATGAGCTGGAGATG
BOK-RP	CCTTGCCCCACGTGATG

Chromatin immunoprecipitation. Cells were fixed with 1% formaldehyde at room temperature, followed by the addition of L-glycine at a final concentration 0.125 M to stop formaldehyde cross-linking. The cells were then washed with 1× PBS and resuspended in cell lysis buffer (pH 8.1) containing 1% SDS, 10 mM EDTA, and 50 mM Tris supplemented with protease and phosphatase inhibitor cocktails. Cell lysates were then subjected to extensive sonication to break chromatin. After centrifugation, the cell lysates are diluted with EBC buffer at a 1:5 ratio. To preclear the cell lysates, samples were incubated with sheared salmon sperm DNA and protein A/G-beads. Immunoprecipitation was performed by incubation with 2 μg of antibody at 4°C overnight in the presence of sheared salmon sperm DNA. Protein A/G-beads were then added to the mixture, followed by further incubation for 1 h. The beads were removed by centrifugation and washed twice with RIPA buffer at 4°C and twice with RIPA buffer containing 500 mM NaCl at 4°C. For the reChIP experiment, after the first immunoprecipitation and wash, the beads were incubated with 75 μl of the first extraction buffer containing 10 mM Tris-HCl (pH 8.0), 2 mM EDTA, and 10 mM DTT at 37°C for 30 min. After centrifugation, the eluent was then diluted 20-fold with cold EBC buffer for the second immunoprecipitation. After a wash with cold RIPA buffer for three times, the beads were then extracted with a solution containing 1% SDS and 0.1 M $NaHCO_3$. The eluted solutions were combined, and 6 M NaCl was added to a final concentration 0.3 M. To reverse cross-linking, samples were heated at 65°C for 5 h. After purification of DNA fragments by using a spin column (Qiagen QuickSpin kit), DNA samples were analyzed by real-time quantitative PCR or by PCRs, followed by agarose gel electrophoresis. The primer sequences used for ChIP are shown in Table 4.

Fluorescence-activated cell sorter analysis. For cell cycle analysis, cells were trypsinized and washed with cold PBS. The cells were then fixed by resuspending in 75% ethanol on ice for 30 min. The cells were then centrifuged and incubated with PBS containing 250 μg/ml RNase A and 30 μg/ml

TABLE 4 Primers used for quantitative real-time PCR

Primer	Sequence (5′–3′)
BIM_ChIP_FP	CCTCTGTCTCTTAGGGCGAC
BIM_ChIP_RP	GTCTTTGAGCTCTCCTCCCTC
BMF_ChIP_FP	ATTCCGACCACCACGCGATA
BMF_ChIP_RP	GGCCCTTTTGACACATTCCC
Bcl-2_ChIP_FP	GGGAATCGATCTGGAAATCCTC
Bcl-2_ChIP_RP	CCCATCAATCTTCAGCACTCT
BAD_ChIP_FP	CGCCCGCCTTTACTTGTAT
BAD_ChIP_RP	TTTCTTCAGAGACCGAGGGA

propidium iodide at room temperature for 30 min. Cell samples were subjected to FACS analysis. For apoptosis analysis, the supernatant (floating apoptotic cells) and the adherent cells were collected and washed twice with PBS. The cell pellet was then resuspended in binding buffer and stained with FITC-PI for 15 min at room temperature. Samples were immediately analyzed by FACS.

Mouse xenograft model. Nude female mice were purchased from Beijing Vital River and received standard institutional care. To prepare cells for nude-mouse injection, SKBR3 cells were infected with lentivirus containing shDHX33 or scramble as a negative control. The cells were trypsinized and resuspended with PBS of a final concentration 10^8 cells/ml. Five-week-old nude mice were subjected to subcutaneous injection with 10^7 cells along their flank, with sample sizes of five mice per condition. When the tumors reached 0.5 cm in diameter, the mice were sacrificed, and the tumors were dissected for photography.

Statistical analysis. Data are presented as means ± the standard deviations (SD). Statistical significance was determined using the Student *t* test, with a *P* value of <0.05 considered significant.

ACKNOWLEDGMENT

We thank members of the Zhang lab for technical input and suggestions and the staff of the Department of Biology at SUSTech, who provided support.

This study was supported by the Science and Technology Innovation Committee of Shenzhen Municipality (grant JCYJ20170307110713487 to Y.Z.) and by the Guangdong Provincial Science and Technology Department (grant 2017A020211024 to Y.Z.).

We declare that we have no competing financial interests.

REFERENCES

1. Bourgeois CF, Mortreux F, Auboeuf D. 2016. The multiple functions of RNA helicases as drivers and regulators of gene expression. Nat Rev Mol Cell Biol 17:426–438. https://doi.org/10.1038/nrm.2016.50.
2. Putnam AA, Jankowsky E. 2013. DEAD-box helicases as integrators of RNA, nucleotide, and protein binding. Biochim Biophys Acta 1829:884–893. https://doi.org/10.1016/j.bbagrm.2013.02.002.
3. Linder P, Jankowsky E. 2011. From unwinding to clamping: the DEAD box RNA helicase family. Nat Rev Mol Cell Biol 12:505–516. https://doi.org/10.1038/nrm3154.
4. Fuller-Pace FV. 2013. DEAD box RNA helicase functions in cancer. RNA Biol 10:121–132. https://doi.org/10.4161/rna.23312.
5. Sarkar M, Ghosh MK. 2016. DEAD box RNA helicases: crucial regulators of gene expression and oncogenesis. Front Biosci 21:225–250.
6. Mitoma H, Hanabuchi S, Kim T, Bao M, Zhang Z, Sugimoto N, Liu YJ. 2013. The DHX33 RNA helicase senses cytosolic RNA and activates the NLRP3 inflammasome. Immunity 39:123–135. https://doi.org/10.1016/j.immuni.2013.07.001.
7. Zhang Y, Forys JT, Miceli AP, Gwinn AS, Weber JD. 2011. Identification of DHX33 as a mediator of rRNA synthesis and cell growth. Mol Cell Biol 31:4676–4691. https://doi.org/10.1128/MCB.05832-11.
8. Fraile JM, Campos-Iglesias D, Rodríguez F, Astudillo A, Vilarrasa-Blasi R, Verdaguer-Dot N, Prado MA, Paulo JA, Gygi SP, Martín-Subero JI, Freije JMP, López-Otín C. 2018. Loss of the deubiquitinase USP36 destabilizes the RNA helicase DHX33 and causes preimplantation lethality in mice. J Biol Chem 293:2183–2194. https://doi.org/10.1074/jbc.M117.788430.
9. Zhang Y, You J, Wang X, Weber J. 2015. The DHX33 RNA helicase promotes mRNA translation initiation. Mol Cell Biol 35:2918–2931. https://doi.org/10.1128/MCB.00315-15.
10. Fu J, Liu Y, Wang X, Yuan B, Zhang Y. 2017. Role of DHX33 in c-Myc-induced cancers. Carcinogenesis 38:649–660. https://doi.org/10.1093/carcin/bgx041.
11. Yuan B, Wang X, Fan C, You J, Liu Y, Weber JD, Zhong H, Zhang Y. 2016. DHX33 transcriptionally controls genes involved in the cell cycle. Mol Cell Biol 36:2903–2917. https://doi.org/10.1128/MCB.00314-16.
12. Tian QH, Zhang MF, Luo RG, Fu J, He C, Hu G, Zeng JS. 2016. DHX33 expression is increased in hepatocellular carcinoma and indicates poor prognosis. Biochem Biophys Res Commun 473:1163–1169. https://doi.org/10.1016/j.bbrc.2016.04.033.
13. Wang H, Yu J, Wang X, Zhang Y. 2019. The RNA helicase DHX33 is required for cancer cell proliferation in human glioblastoma and confers resistance to PI3K/mTOR inhibition. Cellular Signalling 54:170–178. https://doi.org/10.1016/j.cellsig.2018.12.005.
14. Zhang Y, Saporita AJ, Weber JD. 2013. P19ARF and RasV(1)(2) offer opposing regulation of DHX33 translation to dictate tumor cell fate. Mol Cell Biol 33:1594–1607. https://doi.org/10.1128/MCB.01220-12.
15. Czabotar PE, Lessene G, Strasser A, Adams JM. 2014. Control of apoptosis by the BCL-2 protein family: implications for physiology and therapy. Nat Rev Mol Cell Biol 15:49–63. https://doi.org/10.1038/nrm3722.
16. Adams JM, Cory S. 2007. The Bcl-2 apoptotic switch in cancer development and therapy. Oncogene 26:1324–1337. https://doi.org/10.1038/sj.onc.1210220.
17. Letai A, Bassik MC, Walensky LD, Sorcinelli MD, Weiler S, Korsmeyer SJ. 2002. Distinct BH3 domains either sensitize or activate mitochondrial apoptosis, serving as prototype cancer therapeutics. Cancer Cell 2:183–192. https://doi.org/10.1016/S1535-6108(02)00127-7.
18. Touzeau C, Maciag P, Amiot M, Moreau P. 2018. Targeting Bcl-2 for the treatment of multiple myeloma. Leukemia 32:1899–1907. https://doi.org/10.1038/s41375-018-0223-9.
19. Loupakis F, Pollina L, Stasi I, Ruzzo A, Scartozzi M, Santini D, Masi G, Graziano F, Cremolini C, Rulli E, Canestrari E, Funel N, Schiavon G, Petrini I, Magnani M, Tonini G, Campani D, Floriani I, Cascinu S, Falcone A. 2009. PTEN expression and KRAS mutations on primary tumors and metastases in the prediction of benefit from cetuximab plus irinotecan for patients with metastatic colorectal cancer. J Clin Oncol 27:2622–2629. https://doi.org/10.1200/JCO.2008.20.2796.
20. Wajapeyee N, Britto R, Ravishankar HM, Somasundaram K. 2006. Apoptosis induction by activator protein 2α involves transcriptional repression of Bcl-2. J Biol Chem 281:16207–16219. https://doi.org/10.1074/jbc.M600539200.
21. Hilger-Eversheim K, Moser M, Schorle H, Buettner R. 2000. Regulatory roles of AP-2 transcription factors in vertebrate development, apoptosis and cell cycle control. Gene 260:1–12. https://doi.org/10.1016/S0378-1119(00)00454-6.
22. Chazaud C, Oulad-Abdelghani M, Bouillet P, Décimo D, Chambon P, Dollé P. 1996. AP-2.2, a novel gene related to AP-2, is expressed in the forebrain, limbs and face during mouse embryogenesis. Mech Dev 54:83–94. https://doi.org/10.1016/0925-4773(95)00463-7.
23. Mitchell PJ, Wang C, Tjian R. 1987. Positive and negative regulation of transcription *in vitro*: enhancer-binding protein AP-2 is inhibited by SV40 T antigen. Cell 50:847–861. https://doi.org/10.1016/0092-8674(87)90512-5.
24. Moser M, Imhof A, Pscherer A, Bauer R, Amselgruber W, Sinowatz F, Hofstadter F, Schule R, Buettner R. 1995. Cloning and characterization of a second AP-2 transcription factor: AP-2β. Development 121:2779–2788.
25. Oulad-Abdelghani M, Bouillet P, Chazaud C, Dollé P, Chambon P. 1996. AP-2.2: a novel AP-2-related transcription factor induced by retinoic acid during differentiation of P19 embryonal carcinoma cells. Exp Cell Res 225:338–347. https://doi.org/10.1006/excr.1996.0184.
26. Williams T, Tjian R. 1991. Analysis of the DNA-binding and activation properties of the human transcription factor AP-2. Genes Dev 5:670–682. https://doi.org/10.1101/gad.5.4.670.
27. Williams T, Admon A, Luscher B, Tjian R. 1988. Cloning and expression of

AP-2, a cell-type-specific transcription factor that activates inducible enhancer elements. Genes Dev 2:1557–1569. https://doi.org/10.1101/gad.2.12a.1557.
28. Moser M, Ruschoff J, Buettner R. 1997. Comparative analysis of AP-2α and AP-2β gene expression during murine embryogenesis. Dev Dyn 208:115–124. https://doi.org/10.1002/(SICI)1097-0177(199701)208:1<115::AID-AJA11>3.0.CO;2-5.
29. Schorle H, Meier P, Buchert M, Jaenisch R, Mitchell PJ. 1996. Transcription factor AP-2 essential for cranial closure and craniofacial development. Nature 381:235–238. https://doi.org/10.1038/381235a0.
30. Zhang J, Hagopian-Donaldson S, Serbedzija G, Elsemore J, Plehn-Dujowich D, McMahon AP, Flavell RA, Williams T. 1996. Neural tube, skeletal and body wall defects in mice lacking transcription factor AP-2. Nature 381:238–241. https://doi.org/10.1038/381238a0.
31. Moser M, Pscherer A, Roth C, Becker J, Mucher G, Zerres K, Dixkens C, Weis J, Guay-Woodford L, Buettner R, Fassler R. 1997. Enhanced apoptotic cell death of renal epithelial cells in mice lacking transcription factor AP-2β. Genes Dev 11:1938–1948. https://doi.org/10.1101/gad.11.15.1938.
32. Garcia MA, Campillos M, Ogueta S, Valdivieso F, Vazquez J. 2000. Identification of amino acid residues of transcription factor AP-2 involved in DNA binding. J Mol Biol 301:807–816. https://doi.org/10.1006/jmbi.2000.4019.
33. Raap M, Gronewold M, Christgen H, Glage S, Bentires-Alj M, Koren S, Derksen PW, Boelens M, Jonkers J, Lehmann U, Feuerhake F, Kuehnle E, Gluz O, Kates R, Nitz U, Harbeck N, Kreipe HH, Christgen M. 2018. Lobular carcinoma in situ and invasive lobular breast cancer are characterized by enhanced expression of transcription factor AP-2β. Lab Invest 98:117–129. https://doi.org/10.1038/labinvest.2017.106.
34. Turner BC, Zhang J, Gumbs AA, Maher MG, Kaplan L, Carter D, Glazer PM, Hurst HC, Haffty BG, Williams T. 1998. Expression of AP-2 transcription factors in human breast cancer correlates with the regulation of multiple growth factor signaling pathways. Cancer Res 58:5466–5472.
35. Li Z, Xu X, Luo M, Hao J, Zhao S, Yu W, Xiao X, Wu J, Zheng F, Chen M, Li Y, Qin G, Liao Y, Zhao X, Yu X, Guo W, Zou L, Deng W. 2018. Activator protein-2β promotes tumor growth and predicts poor prognosis in breast cancer. Cell Physiol Biochem 47:1925–1935. https://doi.org/10.1159/000491463.